

Copyright WILEY-VCH Verlag GmbH & Co. KGaA, 69469 Weinheim, Germany, 2016.

Supporting Information

Photoacoustic Imaging of Embryonic Stem Cell-Derived Cardiomyocytes in Living Hearts with Semiconducting Polymer-based Ultrasensitive Nanoparticles

Xulei Qin,[†] Haodong Chen,[†] Huaxiao Yang,[†] Haodi Wu, Xin Zhao, Huiyuan Wang, Tony Chour, Evgenios Neofytou, Dan Ding, Heike Daldrup-Link, Sarah C. Heilshorn, Kai Li, Joseph C. Wu**

Dr. X. Qin, Dr. H. Chen, Dr. H. Yang, Dr. H. Wu, Dr. X. Zhao, Mr. T. Chour, Dr. E. Neofytou, Prof. J. C. Wu
Stanford Cardiovascular Institute, Stanford, CA, 94305, United States

Dr. H. Wang, Prof. S. C. Heilshorn
Department of Materials Science and Engineering, Stanford, CA, 94305, United States

Prof. D. Ding
State Key Laboratory of Medicinal Chemical Biology, College of Life Sciences, Nankai University, China, 300071

Prof. H. E. Daldrup-Link, Dr. K. Li
Department of Radiology, Stanford, CA, 94305, United States

Dr. K. Li
Institute of Materials Science and Engineering, A*STAR, Singapore, 138634

Prof. J. C. Wu
Department of Medicine, Division of Cardiology, Stanford, CA, 94305, United States.

[†]Authors (X.Q., H.C. and H.Y.) contributed equally to this study.

*Address correspondence: Joseph C. Wu, 265 Campus Drive G1120B, Stanford, CA 94305-5454, Email: joewu@stanford.edu or Kai Li, Email: likai@imre.a-star.edu.sg

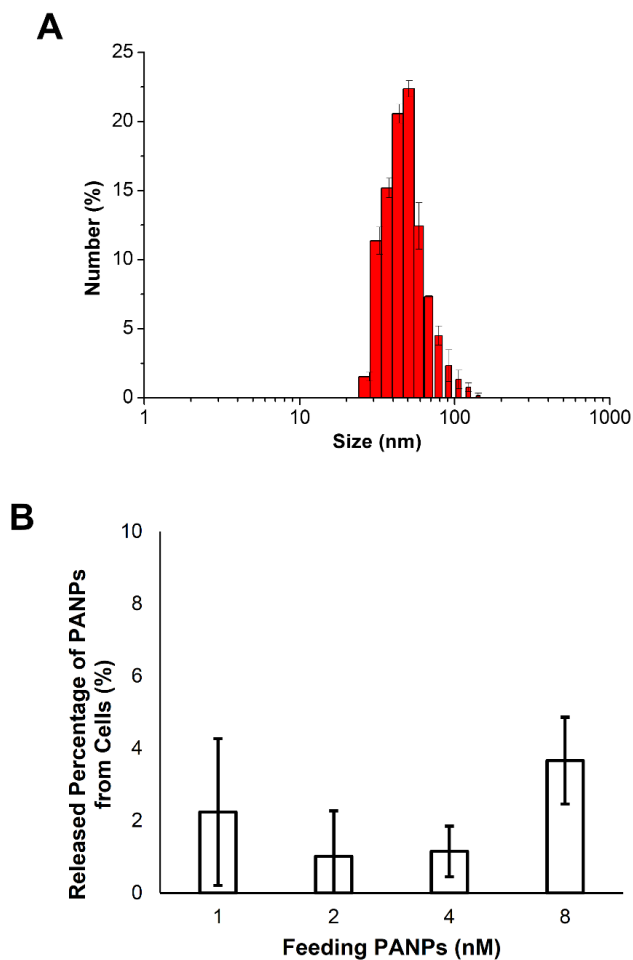


Figure S1. Storage stability of PANPs and their release rates after labeling. (A) The PANPs showed stable sizes (50.8 ± 2.5 nm) even after storage at 4 °C for 1 year. (B) Post-labeling, the release ratios of PANPs from the labeled cells were all below 5% under different feeding PANP doses (1 nM, 2 nM, 4 nM, and 8 nM).

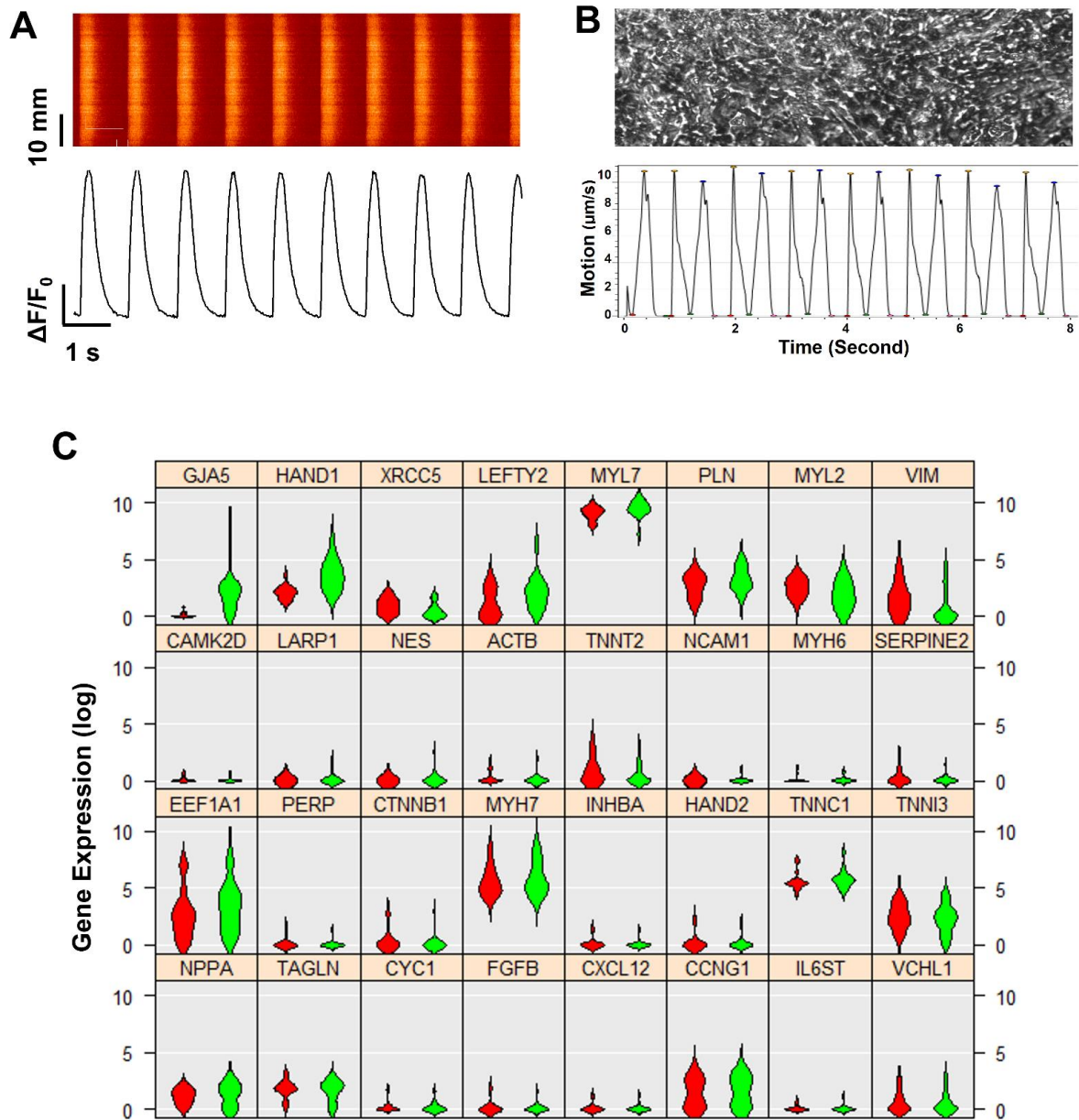


Figure S2. *In vitro* assessment of cell functions and gene expression of PANP-labeled hESC-CMs. (A-B). Calcium handling and contractility of hESC-CMs were analyzed by calcium imaging and motion tracking, respectively. (C) Violin plot showing the distribution of gene expression level for both control (left violin, red) and PANP-labeled cells (right violin, green). Among the 48 genes we examined using microfluidic qPCR, 15 of them had no amplification due to low or no expression (18S rRNA was used as internal reference for RNA loading control). Except for the upregulation of GJA5 and HAND1 following PANP labeling, the remaining 30 genes showed no significant differences between control and labelled cells. N = 17 for each group.

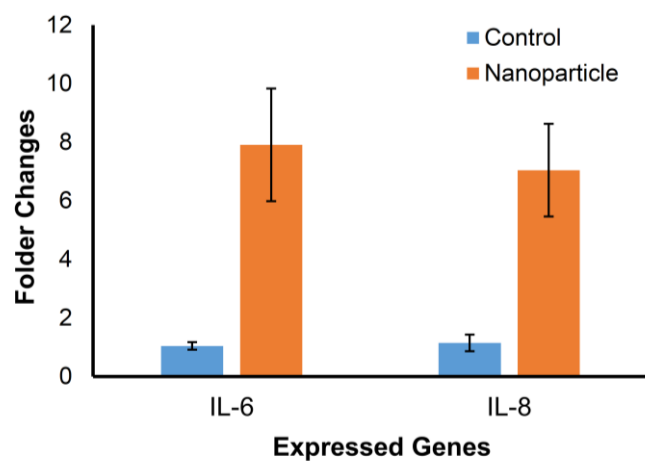


Figure S3. Up-regulated gene expression of IL-6 and IL-8 post-nanoparticle labeling. qPCR analysis indicated that the gene expression of IL-6 and IL-8 in PANP-labeled hESC-CMs were significantly increased compared to the control cells.

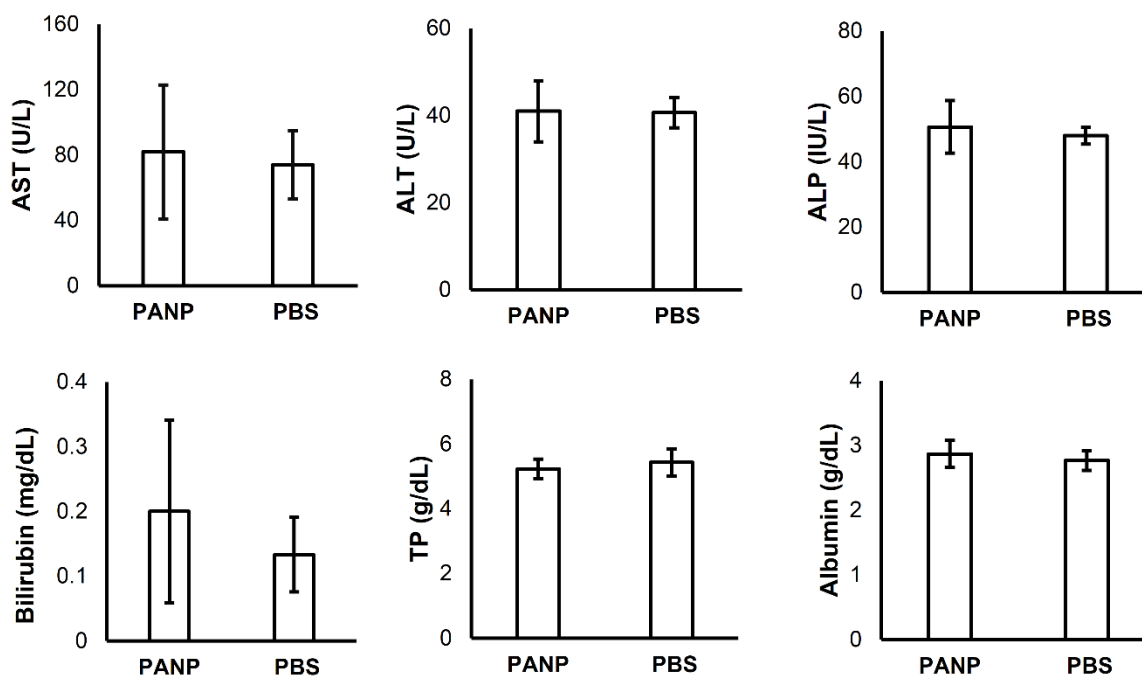


Figure S4. Six biomarkers of blood tests indicate that liver functions of mice are not affected by the intravenously injected PANPs compared to PBS injections. No significant difference is found ($P > 0.05$).

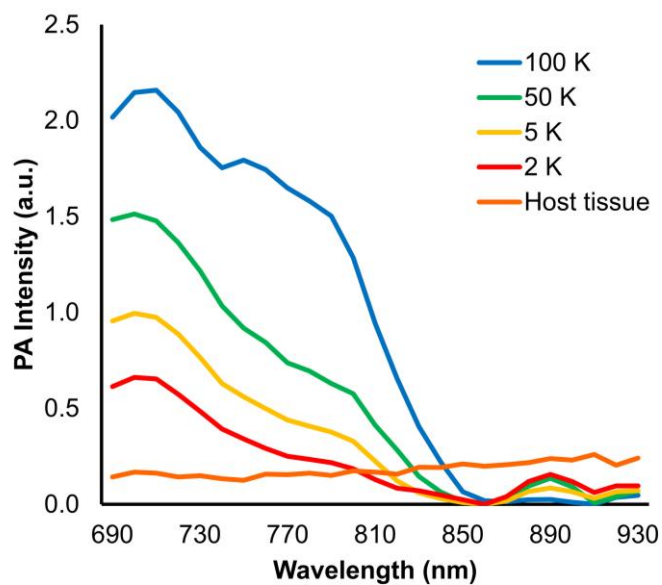


Figure S5. Absolute PA spectra from different numbers of PANP-labeled cells *in vivo*. PANP-labeled cells showed a similar PA spectral pattern, which was different from the PA spectra of background tissues.

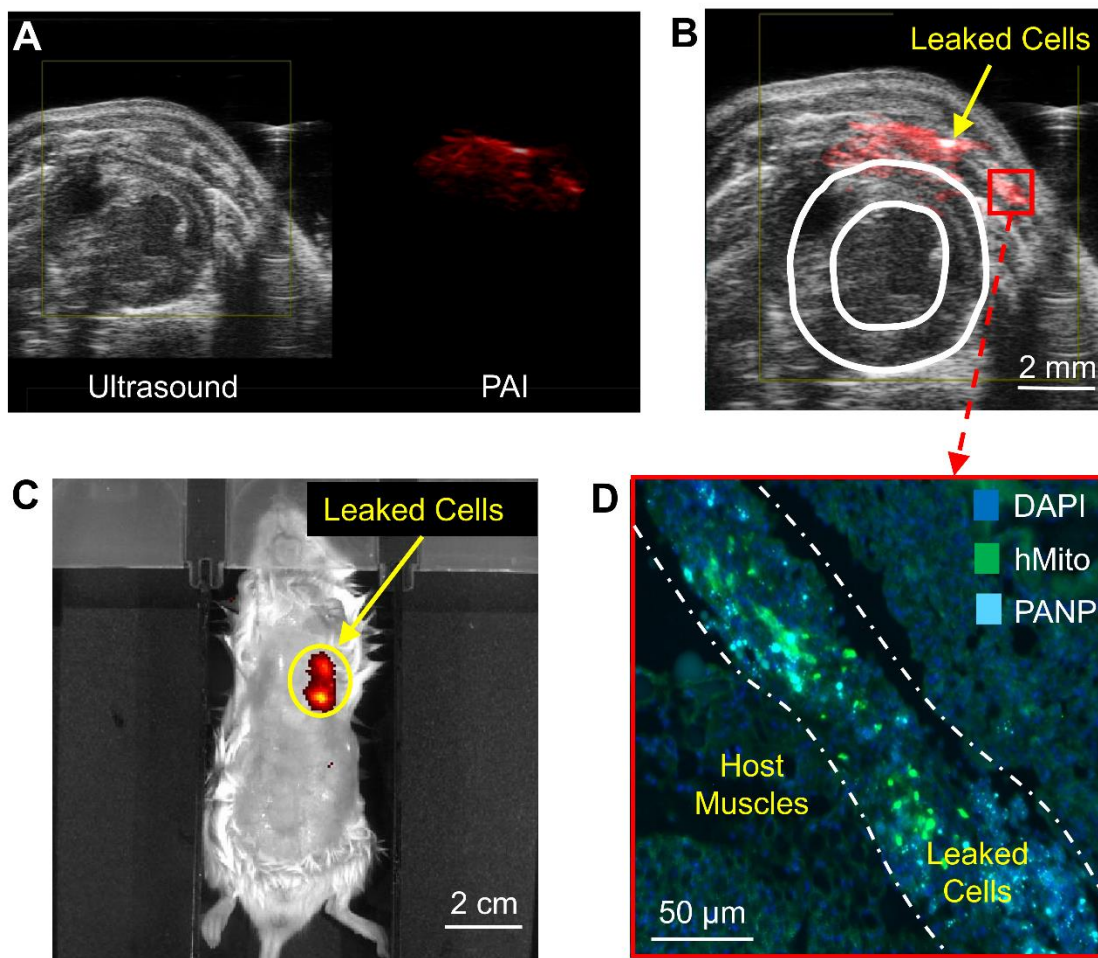


Figure S6. Photoacoustic and ultrasound imaging can detect a failed injection of PANP-labeled cells. (A-B) Photoacoustic and ultrasound imaging and their merged image accurately detected the PANP-labeled cells leaked from a heart. (C) This leaking was difficult to determine from FI. (D) Leaking was confirmed by histological staining with human mitochondrial biomarkers.

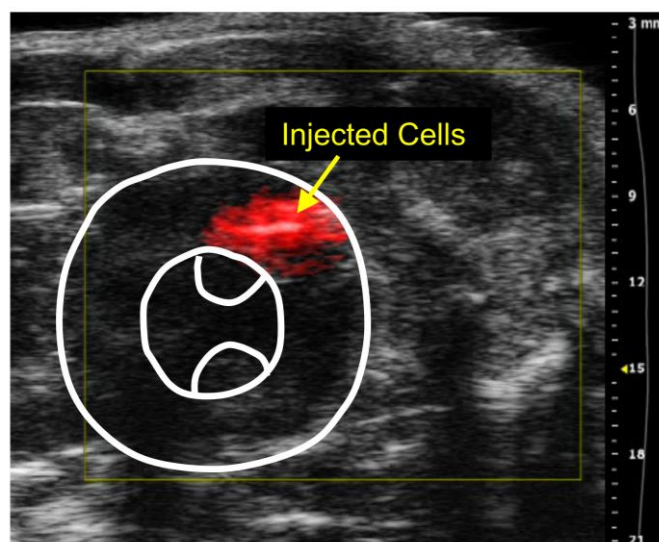


Figure S7. PAI of injected hESC-CMs labeled with PANPs in a rat heart. The yellow arrow indicated the injected cells imaged by PAI while the white lines indicated the myocardium imaged by ultrasound in a rat heart.